Materials Science, Vol. 20, No. 2, 2002

Rare earth complexes in sol-gel glasses*

RENATA REISFELD

Department of Inorganic and Analytical Chemistry, The Hebrew University,
91-904 Jerusalem, Israel, renata@vms.huji.ac.il

The origin of the spectra of rare earth ions arising from f → f and f → d transitions is discussed. The parity-forbidden luminescence of lanthanide ions can be strongly intensified by excitation via molecules characterized by high transition probabilities. Such behaviour opens a route for creation of a class of new sophisticated materials. Luminescent materials based on heteroaromatic lanthanide cryptates are attractive as labels for advanced time-resolved fluoroimmunoassays and molecular markers, their potential use is also conceivable in the field of luminescent displays, molecular photonics and highly luminescent materials in hybrid organic/inorganic glasses. The recent findings of lanthanide complexes trapped in sol-gel inorganic glasses based on silica and zirconia networks are discussed and the theoretical basis of their spectroscopy is presented.

Key words*: rare earths*, *electronic spectra*

1. Electronic spectra of rare earth ions

Rare earth (RE) ions incorporated in a solid or liquid environment show distinct spectral lines of absorption and emission due to the electronic transition within $4f^N$ shell configuration. Figure 1 shows an example partial energy diagram of a RE ion – Eu^{3+} – indicating splitting of the electronic levels due to spin-orbit interaction, which are further split by the ligand field (the *j* splitting). Figure 2 shows a similar diagram for Tb^{3+}.

Since the f orbital is strongly shielded from the outside ligands, the positions of the spectral lines vary only slightly with the environment, however, their intensities are strongly dependent on the host in which the rare earth is embedded [1–3].

The radiative intensities of the trivalent rare earth ions can be easily calculated by the use of Judd–Ofelt theory from the experimentally measured absorption spectra and theoretically calculated matrix element of the ion.

---

*The paper presented at the International Conference on Sol-Gel Materials, SGM 2001, Rokosowo, Poland.

The following approach is applied for f → f transition: the total oscillator strength P of a transition at frequency υ is given by

$$P(aJ;bJ') = \frac{8\pi^2 m\upsilon}{3h(2J+1)}\left[\frac{(n^2+2)^2}{9n}S_{ed} + nS_{md}\right] \tag{1}$$

The connection between integrated absorbance of an electric dipole with line-strength S is:

$$\int k(\lambda)d\lambda = \rho\frac{8\pi^3 m\upsilon}{3hc(2J+1)}\frac{1}{n}\frac{(n^2+2)^2}{9}S_{ed} \tag{2}$$

where $k(\lambda)$ is the absorption coefficient at the wavelength λ, ρ is the RE ion concentration, λ is the mean wavelength of the absorption band, J is the total angular momentum of the initial level and $n = n(\lambda)$ is the bulk index of refraction at wavelength λ. The factor $(n^2 + 2)^2/9$ represents the local field correction for the ion in a dielectric medium.

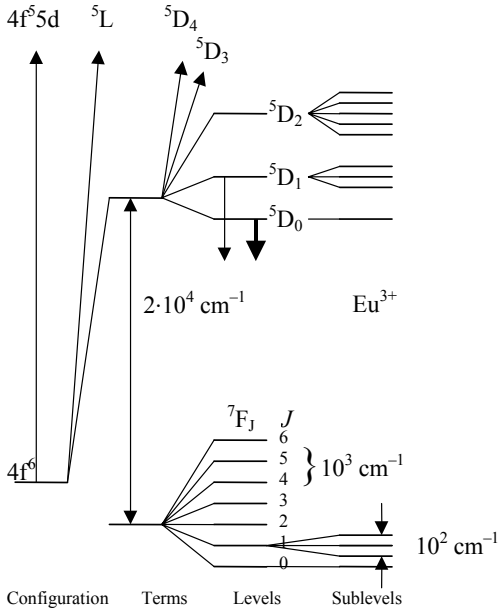

Fig. 1. Partial energy diagram for Eu(III) ion

The spontaneous emission rate is

$$A(aJ;bJ') = \frac{64\pi^4\upsilon^3}{3hc^2(2J+1)}\left[\frac{n(n^2+2)^2}{9}S_{ed} + nS_{md}\right] \tag{3}$$

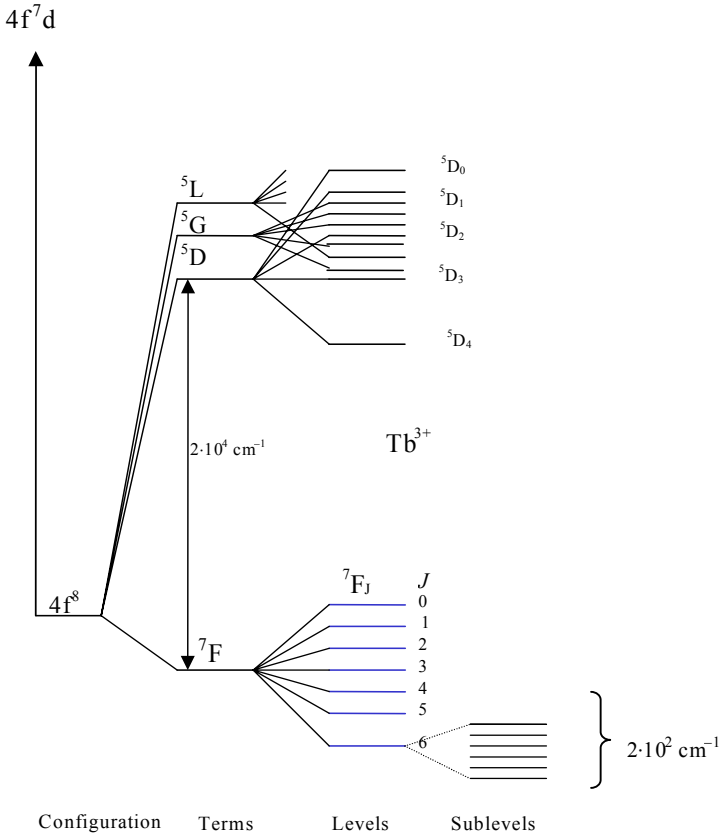

Fig. 2. Partial energy diagram for Tb^{3+} ion

in the case of electric dipole emission Eq. (3) takes the form of:

$$A(aJ;bJ') = \frac{64\pi\upsilon^3}{3hc^2(2J+1)}\left[\frac{n(n^2+2)^2}{9}\right] e^2 \sum_{t=2,4,6} \Omega_t |< (S,L)J \,||\, U^{(t)} \,||\, (S',L'J' >|^2 \quad (4)$$

where Ω is the Judd–Offelt parameter, n is the index of refraction of the matrix. The integrated absorption cross-section is related to the oscillator strength by:

$$\int \sigma(\overline{\upsilon})\, d\overline{\upsilon} = \frac{\pi e^2}{mc^2} P \quad (5)$$

where $\overline{\upsilon}$ is measured in inverse centimeters. For a Lorentzian line

$$\sigma(\upsilon) = \frac{\sigma_0}{1 + \frac{4(\upsilon - \upsilon_0)^2}{(\Delta\upsilon)^2}} \tag{6}$$

where $\Delta\upsilon$ is the full width at the half maximum, υ_0 is the frequency at the peak, and σ_0 is the peak cross-section. Then:

$$\int \sigma(\upsilon) d\upsilon = \frac{\pi}{2} \sigma_0 \Delta\upsilon \tag{7}$$

$$\sigma_0 = \frac{2e^2}{mc^2 \Delta\upsilon} P \tag{8}$$

Thus, for a given linewidth, the peak cross-section for stimulated emission is proportional to the oscillator strength. Equation (8) also shows the importance of the line width $\Delta\upsilon$ in the determination of the cross-section.

The peak induced emission cross-section is related to the radiative probability by the equation:

$$\sigma(\lambda p) = \frac{\lambda p^4}{8\pi c n^2 \Delta\lambda_{eff}} aJ : bJ' \tag{9}$$

where the effective line width $\Delta\lambda_{\text{eff}}$ is used, since for glasses the absorption and emission bands are characteristically asymmetrical.

The cross-section may also be written as:

$$\sigma_p \Delta\overline{\upsilon} = \int \sigma(\overline{\upsilon}) d\overline{\upsilon} = \frac{\lambda p^2}{8\pi c n^2} A(aJ; bJ') \tag{10}$$

The radiative lifetime of level J can be expressed in terms of the spontaneous emission probabilities as:

$$\tau_J^{-1} = \sum_{J'} A(J, J') \tag{11}$$

where the summation is over all terminal levels J'. The fluorescence-branching ratio from level J to J'' is given by

$$\beta_{JJ''} = \frac{A(J, J')}{\sum_{J'} A(J, J')} \tag{12}$$

In addition to the spectroscopic properties, the Judd–Ofelt intensity parameters can also be used to estimate excited-state absorption and the probability of ion-ion interactions that enter into energy-transfer and fluorescence-quenching phenomena.

2. Relaxation processes in trivalent Re

Relaxation processes in trivalent Re include ion-ion energy transfer which can give rise to concentration quenching and non-exponential decay and relaxation by multiphonon emission which is usually essential to complete the overall scheme and can affect the quantum efficiency.

For low concentration of rare earth dopant ions, nonradiative decay mechanism is a multiphonon emission. The results of the theory of multiphonon emission in amorphous materials were recently summarized [4].

The *ab initio* calculation of the transition rate between two electronic states with the emission of p phonons involves a very complicated sum over phonon modes and intermediate states. Due to this complexity, these sums are extremely difficult to compute; however, it is just this complexity which permits a very simple phenomenological theory to be used. There are extremely large numbers of ways in which p phonons can be emitted and the sums over phonon modes and intermediate states are essentially a statistical average of matrix elements. In the phenomenological approach, it is assumed that the ratio of the p-th and $(p-1)$-th processes will be given by a coupling constant characteristic of the matrix in which the ion is embedded but not dependent on the rare-earth electronic states. For a given lattice at low temperature the spontaneous relaxation rate is given by

$$W(0) = B\mathrm{e}^{\alpha\Delta E} \tag{13}$$

where B and α are characteristic of the host (α is negative). Thus, the graph of the spontaneous rate vs. energy gap will be a straight line when this approach is valid. Figure 3 presents an example of exponential behaviour of decay rate on the energy gap between the emitting level and the next lower level to which the energy decays. Experimental data show that the approach is very good for a large variety of hosts. In this way, all multiphonon rates can be inferred from a few measured rates.

The dominant emission process is the one which requires the least number of phonons to be emitted. The minimum number of phonons required for a transition between states separated by an energy gap ΔE is given by

$$p = \frac{\Delta E}{\hbar\omega_{\max}} \tag{14}$$

where $\hbar\omega_{max}$ is the maximum energy of optical phonons. With increased temperature, stimulated emission of phonons by thermal phonons increases the relaxation rate W according to

$$W(T) = W(O)\,(1 + \overline{n}\,(\hbar\omega_{max}))^{P} \tag{15}$$

where $\overline{n}$ is the average occupation number of phonons of energy $\hbar\omega_{max}$.

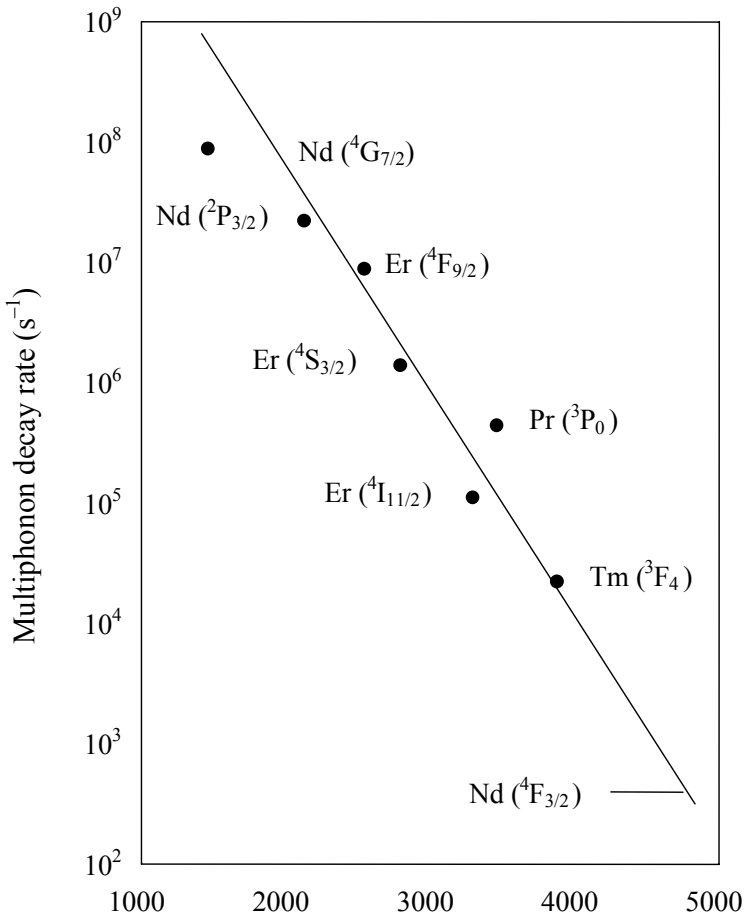

Fig. 3. An example of multiphonon decay for trivalent RE in a silicate glass

The non-radiative relaxation in the rare earth ions is related to their excited states population and is governed by the energy difference between the emitting level and the next lower level, separated by the number of phonons of the host [3, 4].

The presence of water or solvent molecules in the co-ordination sphere of the RE is often responsible for quenching of the luminescence via multiphonon relaxation. Mac-

rocyclic ligands such as cryptates shield the lantanide ion from the solvent preventing the quenching effect. Luminescent properties of co-ordination compounds are widely used in chemical, biological and technological applications [5, 6].

In contrast to the spectra arising from f → f transitions, in all the trivalent rare earth ions having oscillator strength of ~10^{-6}, trivalent Ce^{3+} ion forms an exception as its spectrum arises from f → d transition.

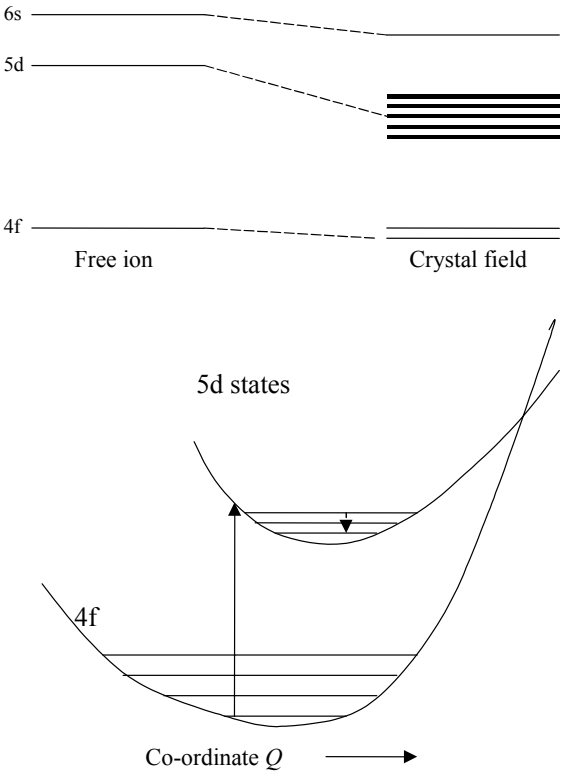

Fig. 4. Electronic levels (upper) and configurational diagram (lower) of Ce^{3+}

Neutral cerium atom has a $ls^2 2s^2 p^6 3s^2 p^6 d^{10} 4s^2 p^6 d^{10} f^2 5s^2 p^6 6s^2$ electronic configuration. In liquids and solids, Ce ions can occur in a trivalent or a tetravalent state, i.e. by losing its two 6s electrons and one or both of its 4f electrons. The trivalent state with a single 4f electrons is optically active; the resulting electronic energy level solids structure is shown in Fig. 4. When cerium enters a liquid or a solid, the expansion of the electron shells decreases the electrostatic interaction between the electrons resulting in a reduction of the energy of the excited states from their free ion values. This nephelauxetic shift increases with the degree of covalency of the cerium–anion bond. The spin-orbit interaction splits the 2f ground into two J states separated by ~2200 cm^{-1}. The (2J + l)-fold degeneracy of these states is reduced by the ligand

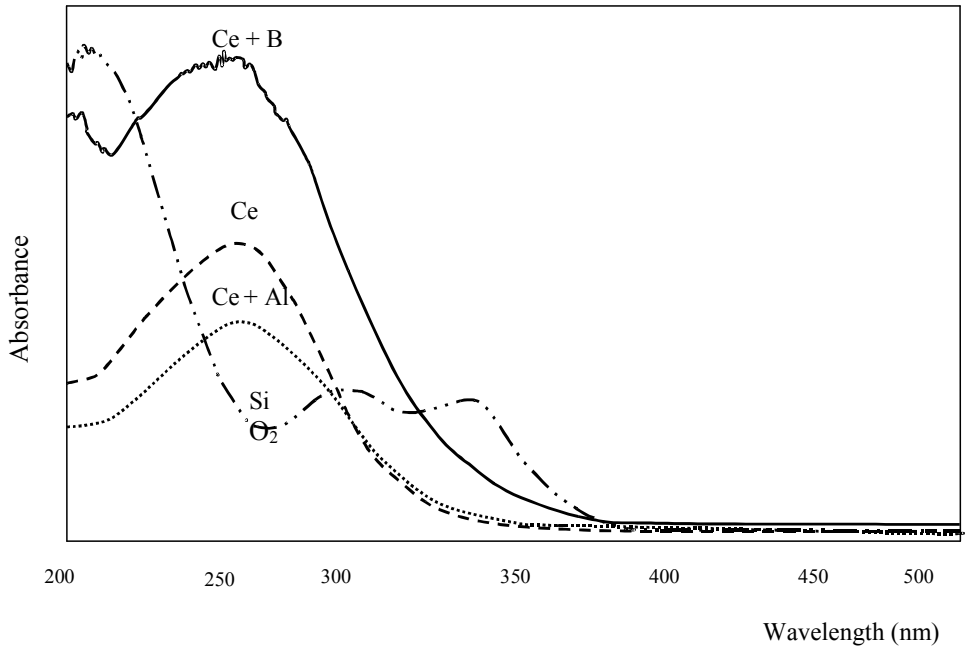

Fig. 5. Absorption spectrum of Ce^{3+} in silica glass prepared by the sol-gel method, the glasses with addition of Al^{3+} and B_2O_3 are also indicated in the figure

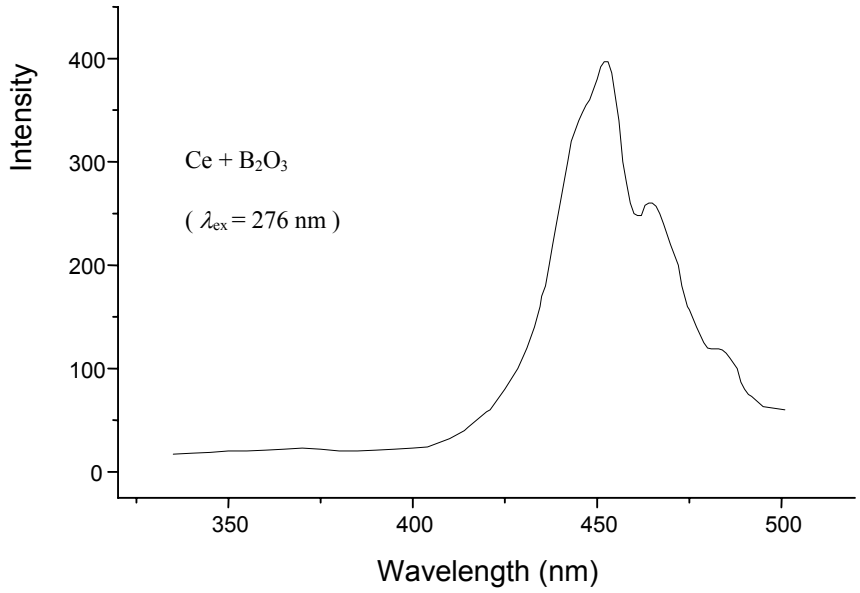

Fig. 6. Luminescent spectrum of Ce^{3+} in sol-gel silica glass with addition of B_2O_3

field. Because the 4f electron is shielded from the ligand field by the closed 5s and 5p electron shells, the overall splitting of the ^2F_j states is small, typically only a few hundred cm^{-1}. When the 4f electron is excited to the outer 5d state, however, it is subjected to the effect of the ligands. Depending upon the site symmetry, the degeneracy of the 5d state is partially or completely removed. The overall splitting of the 5d manifold is typically of the order of 5000–10 000 cm^{-1}.

Electric-dipole transitions between the 4f ground state and the 5d excited state of Ce^{3+} are parity allowed and have large oscillator strengths. Contrary to a long-lived emission of many 4f *j* levels of several lanthanides in glasses and crystals, corresponding to very low (10^{-6}) oscillator strengths Ce^{3+} is the only trivalent lanthanide which in the UV spectrum (Fig. 5) region shows high oscillator strength (0.01–0.1). Figure 6 shows an emission spectrum of Ce^{3+} in glass obtained by the sol-gel method [7].

3. Complexes of rare earths in sol-gel glasses

As described above, electronic transitions in trivalent rare earth ions within the f shell are forbidden by the Laporte rule and the luminescence which is dependent on the absorption of photons to the electronic levels of the same configuration is therefore weak. In addition, there is the possibility of multiphonon relaxation assisted by water or solvent vibration.

Therefore, much effort has been devoted to the study of complexes which contain ligands that have high absorbance in the UV followed by efficient energy transfer to excited f states of RE The required structure of such complex are for instance 3,3′-biisoquinaline-2,2′ dioxide (biq O_2) and biq O_2-cryptate protects also from quenching the RE ions from water vibration [8, 10].

The dominant characteristics which determines the luminescence quantum yield of these complexes are the energy gap law corresponding to the difference in energy between the excited emitting state and the highest state of the ground ^{2s+1}L term, the location and influence of ligand metal charge transfer (LMCT) states, and the competition with non-radiative decay processes. Inter- and intramolecular dynamics also affect the luminescence properties of lanthanide(III) complexes [8]. These are severely reduced in solid samples, and, more recently, in experiments in which the luminescent species have been incorporated into transparent sol-gel [8, 10].

In order to increase inertness and minimize solvent interaction, one can use a system consisting of Eu(III) ions encapsulated not only in cryptand formed by 3,3′-biisoquinaline-2,2′-dioxide and diaza-18-crown-6 groups, but also the cryptate can be entrapped in rigid and porous silica matrix. The matrix can be prepared by the sol-gel process, i.e. two reactions with tetraalkoxysilane or other precursors.

The non-radiative relaxation processes in the rare earth ions are related to their excited state population and are governed by the energy difference between the emitting level and the next lower level, separated by the number of phonons of the host [3, 4].

Silica xerogel doped with $[Eu{\cdot}cryptand]^{3+}$ was prepared by the sol-gel method from a hydrolyzed tetramethoxysilane solution containing $[Eu{\cdot}cryptand](CF_3SO_3)_2Br$. UV-visible optical absorption spectra, fluorescence excitation and emission spectra, fluorescence lifetime as well as luminescence quantum yield were measured. Experiments were carried out in aqueous solutions and in rigid silica xerogels at room temperature. It is shown that the excitation is centred at the ligand, but the metal ion takes part in the emission process. In other words, the antenna effect was observed in the Eu(III) cryptate in the solution and xerogel. The cryptate entrapped in the xerogel showed higher emission efficiency and longer lifetime than in solution [10].

Recently, several studies have been performed on trivalent rare-earth ions doped in SiO_2 gel matrixes via the sol-gel process [11, 12]. Inorganic rare-earth salt chloride or nitrate were used. Only a weak emission can be observed from rare-earth ions doped in SiO_2 prepared at moderate temperature due to non-radiative relaxation originated from the interaction with the hydroxyl ions of water residue [11, 12]. It has been shown that organic complex of rare earth doped in SiO_2 gel had better fluorescence properties with respect to comparable inorganic salts [9, 10]. The implication of this finding is that rare-earth organic complexes doped in sol-gel hosts are good candidates for phosphors, active waveguides, optical sensors and markers of biological molecules [13].

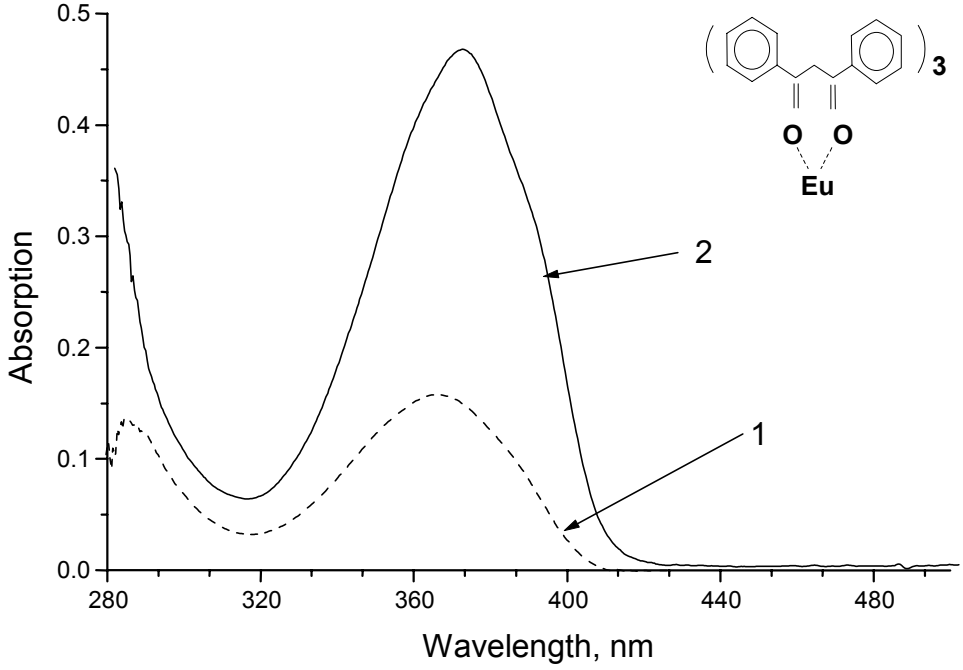

Fig. 7. Absorption spectrum of $Eu(DMB)_3$ complex in zirconia glass and zirconia glymo films

Zirconia glasses have some advantages over silica glasses because of their high stability and low phonon energies [14]; they were found to be excellent materials for incorporation of CdS nanoparticles [15].

Preparation of zirconia and zirconia ormosils and their physical properties have been described in details in [14].

Incorporation of RE ions into zirconia matrix allowed us to obtain better luminescence than in silica matrix [12, 15], however, this luminescence could be greatly increased when Eu^{3+} was incorporated into complexes such as dibenzoylmethane $Eu(DBM)_3$ or into 3,3′biisoquinaline-2,2′dioxide cryptate [13].

The complex $Eu(DBM)_3$ was prepared by Prof. M. Pietraszkiewicz and incorporated into films of zirconia and zirconia glymo in our laboratory. Figure 7 presents the absorption spectra and in Fig. 8 the emission spectra of the complexes are shown. When normalized to the absorption an increase of factor of five is observed in Eu^{3+} luminescence in the glymo films as compared with zirconia glass. For preparation of cryptate in zirconia films the following procedure was used [13].

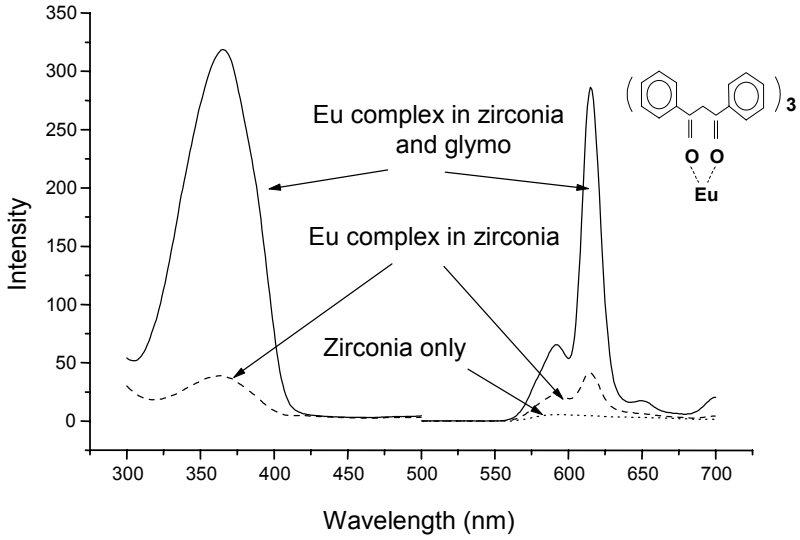

Fig. 8. Excitation and emission spectra of $Eu(DMB)_3$ complex in zirconia and zirconia glymo films

Two zirconia-doped films were prepared: one with Eu(III) cryptate, and a hybrid material obtained by cross-condensation of zirconia tetrapropoxide and 3-glycidoxypropyltrimethoxysilane (abbreviated as *glymo*). The hybrid matrix incorporating silica and organic part was expected to bring two advantages: to bind water via oxirane ring opening, and to provide organic hydrophobic environment advantageous to repel the remaining water molecules from the proximity of the Eu(III) cryptate. The expectation was to enhance the luminescence performance. The Eu^{3+} ions were also prepared in zirconia film for comparison.

Absorption spectra of pure zirconia film and film doped with Eu_2O_3 as well as cryptate in glymo film are presented in Fig. 9. These films were transparent in the range of 350−700 nm, the zirconia-doped with Eu_2O_3 showed a broad and weak band around 350 nm. The samples with Eu cryptate show an intense band at 269 nm belonging to the charge transfer of Eu cryptate complex. It should be noted that the charge transfer of Eu oxide is positioned in the same spectral range, however, its intensity is negligible compared with the complex prepared with the same concentration of Eu.

Both Eu cryptate in zirconia and in zirconia-glymo contain a band with a maximum at 350 nm characteristic of the heterocyclic ligand absorbance. The intensity in both cases is the same within the experimental error. Therefore, there is no evident influence of glymo on electronic spectra of the cryptate unlike in $Eu(DBM)_3$ complex.

In Figure 10, the excitation and emission spectra of the complex in zirconia–glymo (upper) and zirconia thin films (lower) excited at 350 nm and 269 nm is presented. The emission spectra consist of several bands at 590 nm ($^5D_0 \rightarrow {}^7F_1$), 617nm ($^5D_0 \rightarrow {}^7F_2$) (the most intense), 647nm ($^5D_0 \rightarrow {}^7F_3$) and 684 nm ($^5D_0 \rightarrow {}^7F_4$).

The incorporation of the cryptate complexes into zirconia films results in dramatic increase of the emission intensity as well as in the increase of the absorption intensity of Eu. The former results form the shielding of OH vibrations responsible for the non-radiative relaxation and lowering of the symmetry site in which Eu is situated. The most dramatic effect must arise from energy transfer from the organic ligand to the Eu^{3+} as depicted in Fig. 11.

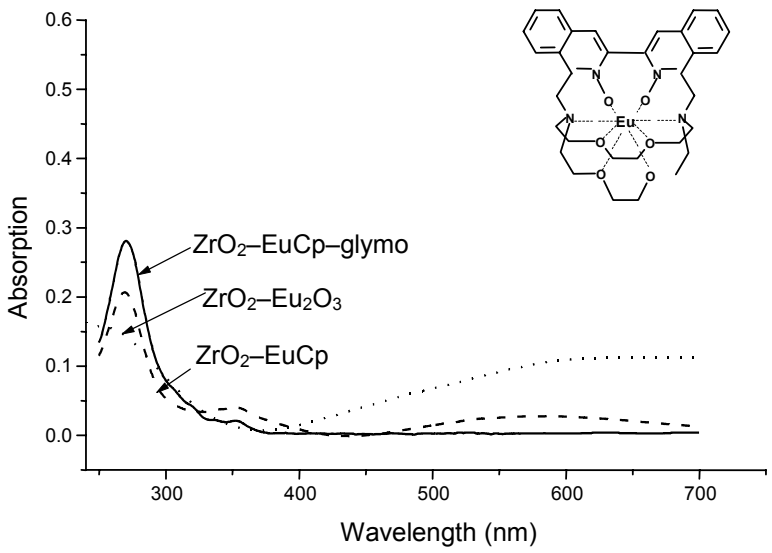

Fig. 9. Absorption spectrum of Eu^{3+} in zirconia films compared to absorption of europium cryptate in zirconia and glymo

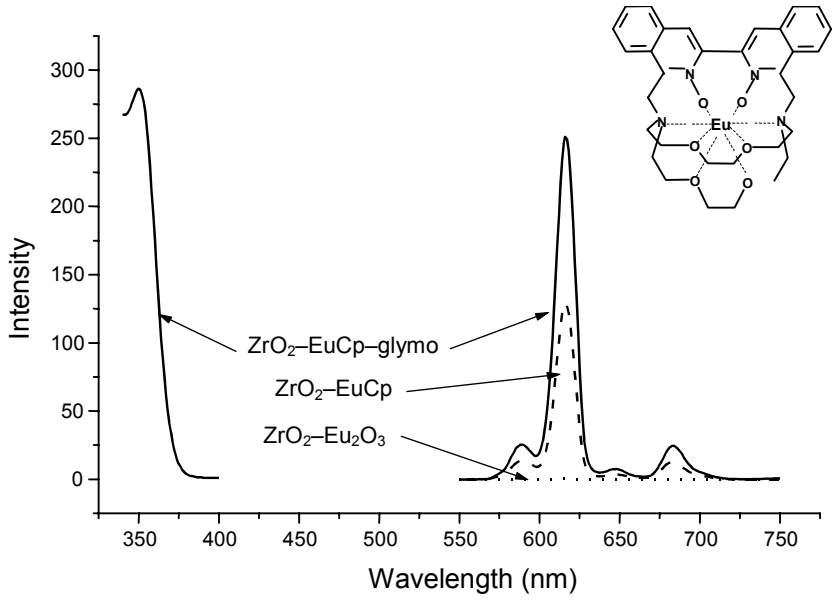

Fig. 10. Emission spectrum of Eu in ZrO_2 cryptate complex of Eu^{3+} in zirconia and the same complex in glymo

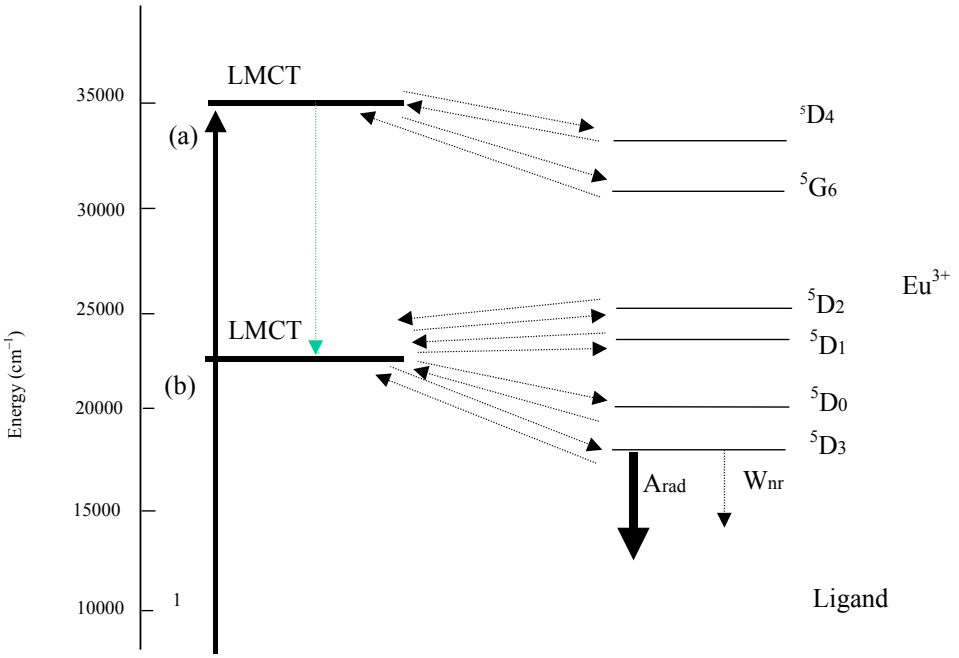

Fig. 11. Diagram of the most probable states in the energy transfer process of the Eu cryptate in sol-gel glass. The LMCT state close to the triplet (a) and the singlet (b) states of the ligand are also presented. Solid and dashed arrows describe radiative and non-radiative process, respectively

The phenomena of increase of transition probabilities are reflected by higher absorption of the complex. The energy-transfer rates between the ligands and the lanthanide ion were calculated recently in a complex of $Eu(bpy{\cdot}bpy{\cdot}bpy)^{3+}$ [9].

The model took into account the molecular structure of the complex and the ligand and the location of ligand with respect to metal states. The energy transfer rate between the ligand and the lanthanide ion were obtained with the model that includes the multipolar and exchange coulands interaction. The very elegant treatment presented there can be used in future for a general case of energy transfer between the cryptate ligand and the lanthanide ion as shown in Fig. 11.

Acknowledgement

The author is very grateful to Professor Marek Pietraszkiewicz for the very fruitful co-operation and discussions on cryptate complexes.

References

[1] JØRGENSEN C.K., REISFELD R., *Chemistry and spectroscopy of rare earths*, [in:] *Topics in Current Chemistry*, 100 (1982), 147.
[2] REISFELD R., Inorg. Chim. Acta, , 95 (1984), 69.
[3] REISFELD R., JORGENSEN C.K., *Excited state phenomena in vitreous materials*, [in:] K.A. Gschneidner, L. Eyring (Eds.), *Handbook on the Physics and Chemistry of Rare Earths*, 9, chapt. 58, North-Holland, Amsterdam (1987), 1.
[4] REISFELD R., *Luminescence and nonradiative processes in porous glasses*, [in:] *Proceedings of Advanced Study Institute on Advances in Nonradiative Processes in Solids*, B. Di Bartolo and Xuesheng Chen (Eds.), Plenum, NATO ASI Series B Physics, 249 (1991), 397.
[5] BÜNZLI J.-C.G., CHOPPIN G.R., *Lanthanide Probes in Life, Chemical and Earth Sciences: Theory and Practice*, Elsevier, 1989.
[6] SABBATINI N., GUARDIGLI M., LEHN J-M., Co-ord. Chem. Rev., 123 (1993), 201.
[7] REISFELD R., MINTI H., PATRA A., GANGULI D., GAFT M., Spectrochimica Acta Part A., 54 (1998), 2143.
[8] LONGO R. et.al., Chemical Physics Letters, 328 (2000), 67.
[9] GAWRYSZEWSKA P.P., PIETRASZKIEWICZ M., RIEHL J.P., LEGENDZIEWICZ J., J. Alloys and Compounds, 300−301 (2000) 283.
[10] CZARNOBAJ K. et al., Spectroscopica Acta, 54 (1998) 2183.
[11] REISFELD R., *Structure and Bonding*, 85 (1996), 215 and references therein.
[12] REISFELD R., ZELNER M., PATRA A., J. of Alloys and Comp., 300 (2000), 147.
[13] SARAIDAROV T., REISFELD R., PIETRASZKIEWICZ M., Chem. Phys. Letters, 330 (2000), 515.
[14] SOREK Y., ZEVIN M., REISFELD R., HURVITS T., RUSCHIN S., Chem. Mater., 9 (1997), 670.
[15] ZELNER M., MINTI H., REISFELD R., COHEN H. TENNE R., Chem. Mater., 9 (1997), 2541.

Received 16 June 2001
Revised 19 December 2001